PHYSICAL REVIEW B VOLUME 37, NUMBER 3 15 JANUARY 1988-II

Calculated optical properties of semiconductors

M. Alouani, L. Brey,* and N. E. Christensen
Max-Planck-Institut für Festkörperforschung, Postfach 80 06 65, D-7000 Stuttgart 80, Federal Republic of Germany
(Received 11 May 1987; revised manuscript received 8 September 1987)

The complex dielectric functions, $\epsilon(\omega)=\epsilon_1(\omega)+\epsilon_2(\omega)$, are calculated for the semiconductors Ge, GaAs, InSb, and CdTe in order to explain new ellipsometric measurements. The dependence on hydrostatic pressure of the dielectric functions of GaAs and Ge is also investigated. The band structures and optical transition matrix elements are obtained from the relativistic self-consistent linear muffin-tin orbitals scheme. In order to correct for the too low values of the gaps as obtained within the local-density approximation, shifts are introduced by adding external potentials that are sharply peaked at the atomic sites. These external potentials are kept invariant under pressure. In general, our calculation enables a consistent assignment of the structure in the experimental spectra and also of the pressure dependence of the peak positions. Our band-structure calculations show that the indirect band gaps of GaAs decrease under pressure at a rate of -1.15 eV/Mbar whereas in the case of Ge both direct and indirect band gaps increase with pressure. These shifts of band gaps are in good agreement with experiment.

I. INTRODUCTION

The electronic structure of diamond- and zinc-blende-type semiconductors has been extensively studied over the last two decades.[1-13] The nonlocal empirical pseudopotential model[2] (EPM) gives a satisfactory interpretation of the optical properties by fitting the pseudopotentials to calculated energy bands[1] or to experimental data.[3-8] Efforts were also made during the last ten years to accurately estimate the local-field correction,[14-19] the excitonic effects,[16-22] and other many-body effects[15,17] in the optical spectrum. It was found that the local-field correction does not shift the peak positions but reduces the intensity of the E_1 and E_2 peaks, leading to a poorer agreement in this energy range with experimental.[14-16] At higher energy the optical spectrum appears to be improved.[14-16] The calculations of the quasiparticle excitation energies of silicon by Wang and Pickett[20] have improved the direct and indirect band gaps. The inclusion of the so-called dynamical effects to the self-energy obtained with the Coulomb-hole-screened exchange gives results for the gaps and band dispersion for elemental semiconductors in good agreement with experimental data[17-19] and also for some zinc-blende-type compounds.[19]

Recently, first-principles nonrelativistic calculations of the optical properties for Si, Ge, GaP, GaAs, ZnS, and ZnSe were reported by Wang and Klein.[23] They used the linear combination of Gaussian orbitals method together with a local-density formulation of the exchange-correlation functional. In general, a good qualitative agreement with experiment was obtained,[23] but all peaks are located too low in energy. This is the usual feature of band structures derived within the local-density approximation (LDA). When, in addition, relativistic effects are included, the comparison[12] to experiment is even less favorable.

The relativistic reduction of the band gaps is due mainly to the downshift of s states, due to the large mass-velocity effects. In order to compensate for the too low gap values, we add, in the present work, "false Darwin shifts" by means of extra, sharply peaked potentials, as described elsewhere.[11] The self-consistent band structures are calculated with the inclusion of these extra potentials, which are chosen so that gaps at three symmetry points (Γ, X, L) approximately match the experimental data. These extra potentials are kept pressure independent.[11]

Our aim in this work is to interpret new ellipsometry measurements of the complex dielectric function and to predict the evolution of the optical spectra of semiconductors under pressure. For this purpose we use the linear muffin-tin orbitals (LMTO) approach in its scalar-relativistic form.[24] As a starting potential for the self-consistency we use the LDA potential, at which we add the previously described external potentials. Under compression these external potentials are kept invariant. The band schemes obtained are directly used to evaluate the imaginary part of the dielectric function under hydrostatic pressure. The use of the external potentials is justified by the fact that until now there has been no first-principles calculation of the dielectric function of the zinc-blende semiconductor type which satisfactorily explains the evolution of the optical spectra under hydrostatic pressure. Although empirical in nature, our correction method has some appealing features, in our opinion. It is made within the spirit of the density-functional theory in the sense that the adjusting potential is added as an external potential in the LDA functional, and the full potential is allowed to adjust to self-consistency.

The method of calculation of the dielectric function of GaAs with and without the adjusting potentials is discussed in Sec. II. The results and discussions of the dielectric functions of four semiconductors and the prediction of the pressure dependence of the dielectric func-

 ©1988 The American Physical Society

tions of GaAs and Ge are given in Sec. III. In Sec. IV we draw the conclusions.

II. METHOD OF CALCULATION

The linear muffin-tin orbitals method (LMTO) which we use in the present study of optical properties of GaAs, Ge, InSb, and CdTe is described elsewhere,[24] and the details of its application to the calculation of the electronic structure of the zinc-blende-type compounds are presented in previous papers.[11-13] The self-consistent potentials are generated by means of *scalar-relativistic* calculations, i.e., all relativistic effects except the *spin-orbit* (s.o.) coupling are included. The so-called "combined correction term"[24] is included, and in the final band-structure calculation the s.o. is added as a formal perturbation term in the Hamiltonian.[24] The band structures obtained with inclusion of adjusting potentials are presented in Figs. 1–4 for GaAs, Ge, InSb, and CdTe, respectively. The self-consistent energy eigenvalues and wave functions are used to determine the complex dielectric function.

In the limit of vanishing linewidth the imaginary part $\epsilon_2(\omega)$ of the dielectric function is given by[25]

$$\epsilon_2(\omega)=\frac{4\pi^2e^2}{3m^2\omega^2}\sum_{n,n'}\int\frac{2}{(2\pi)^3}d^3\mathbf{k}\,|\langle n\mathbf{k}|\mathbf{P}|n'\mathbf{k}\rangle|^2 \times f_n^{\mathbf{k}}(1-f_{n'}^{\mathbf{k}})\delta(E_n^{\mathbf{k}}-E_{n'}^{\mathbf{k}}-\hbar\omega)\ , \quad (1)$$

where $f_n^{\mathbf{k}}$ is the zero-temperature Fermi distribution function for the state $|n\mathbf{k}\rangle$ with band index n and wave vector $\mathbf{k}$. The matrix elements $\langle n\mathbf{k}|\mathbf{P}|n'\mathbf{k}\rangle$ are calculated with the wave function $|n\mathbf{k}\rangle$ expressed in terms of the one-center expansion,[24] except for InSb and CdTe, where we have used the full wave function, as described elsewhere.[26] In the one-center expansion[24] we have found that the intensity of the peaks of the dielectric function of these two compounds is overestimated. The reason for this is related to the fact that InSb and CdTe are ionic semiconductors, and an accurate description of the wave functions in the outer parts of the atomic polyhedra is then particularly important.

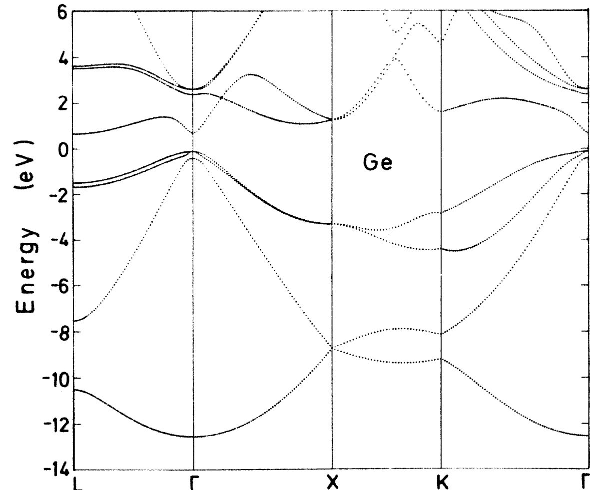

FIG. 2. As in Fig. 1, but for Ge.

Using the Wigner-Eckart theorem, the matrix $\mathbf{P}=\hbar/i\nabla$ can be written in the form of an irreducible tensor of order one.[26] The imaginary part of ϵ, $\epsilon_2(\omega)$, is calculated for photon energies ranging up to 1 Ry. The $\mathbf{k}$-space integration is performed by means of the tetrahedron method[27] based on 95 $\mathbf{k}$ points in the irreducible part of the Brillouin zone (IBZ). The inclusion of more $\mathbf{k}$ points in the IBZ does not produce any significant changes in the spectrum. The real part, $\epsilon_1(\omega)$, is obtained by a Kramers-Kronig transformation of $\epsilon_2(\omega)$ in which a tail of the form $(\beta\omega)/(\omega^2+\gamma^2)^2$, as used by Petroff *et al.*,[28] is attached for energies greater than 13.6 eV, where γ is equal to 4.5 eV and β is determined by continuity of $\epsilon_2(\omega)$ at 13.6 eV.

The dielectric functions calculated for GaAs with and without the extra potentials mentioned above are shown

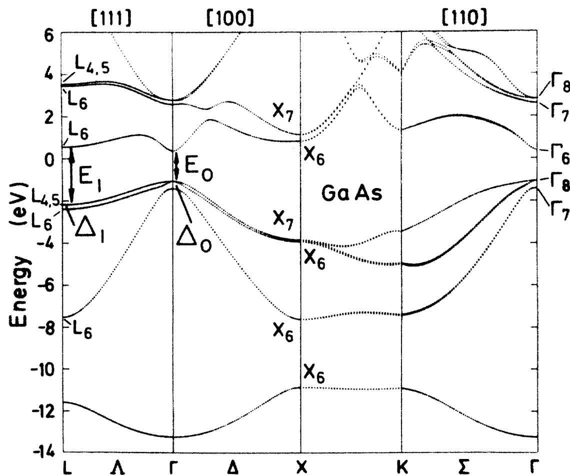

FIG. 1. Equilibrium relativistic self-consistent local-density band structure of GaAs with external-potential correction. Spin-orbit coupling is included.

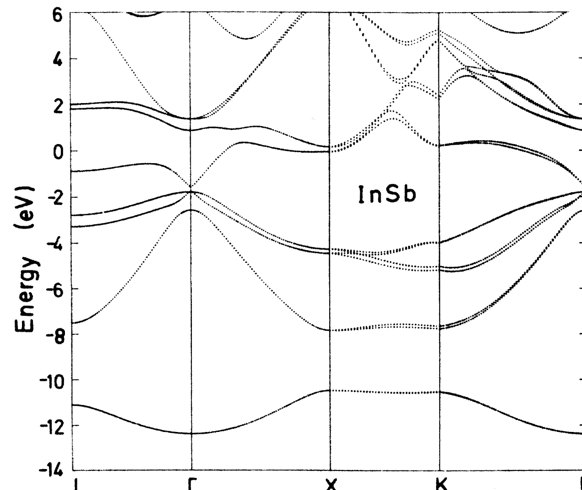

FIG. 3. As in Fig. 1, but for InSb.

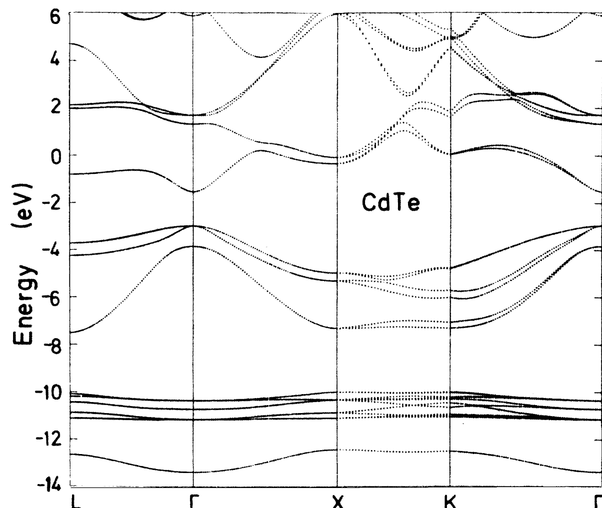

FIG. 4. As in Fig. 1, but for CdTe.

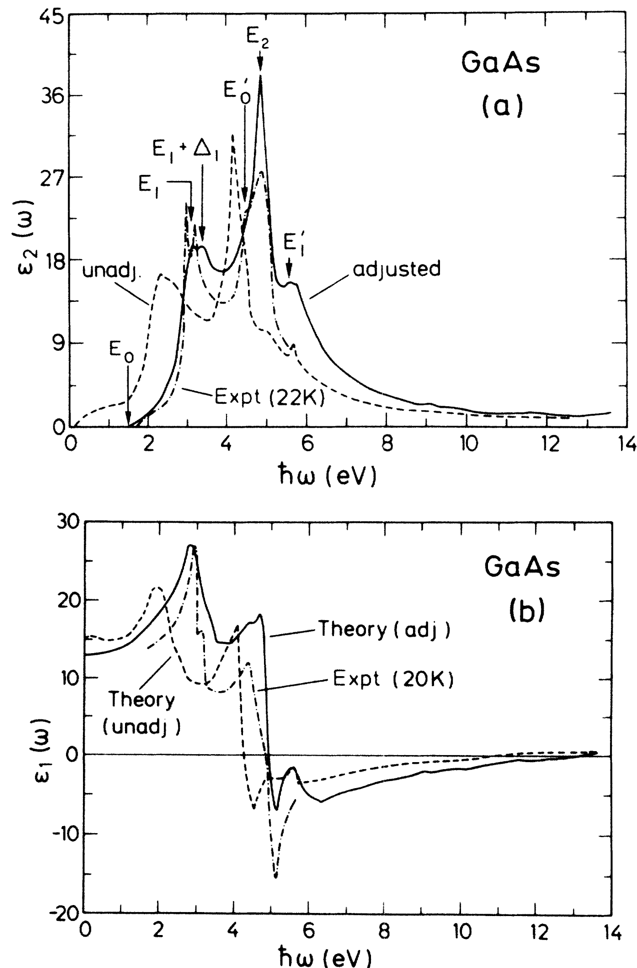

FIG. 5. Dielectric function of GaAs with extra-potential correction EPC (solid curves) and without EPC (dashed curves) compared to the experimental results of Ref. 29 (dash-dotted curves). (a) Imaginary part $e_2(\omega)$; (b) real part $\epsilon_1(\omega)$.

in Fig. 5. We have also presented in this figure the experimental results of Lautenschlager *et al.*[29] (dash-dotted curves). It is seen that the main structures E_1 and E_2 in $\epsilon_2(\omega)$ calculated without correction are located too low in energy when compared to experiment. The inclusion of the extra potentials shifts all the theoretical peaks towards higher energy and this corrected spectrum agrees well with the experiment.[29] In order to illustrate the effects of the matrix elements we compare, in Fig. 6, $\epsilon_2(\omega)$ (with matrix elements) and the joint-density-of-states function (JDS) for GaAs. The peaks present in the JDS at high energy are reduced significantly in the $\epsilon_2(\omega)$ spectrum because the transition probability becomes small at higher energy. Hence, a quantitative comparison to experiment is only meaningful if the matrix elements of **P** are included in the calculation of the $\epsilon_2(\omega)$ spectrum. We further compare, in Fig. 7, our calculated $\epsilon_2(\omega)$ of GaAs with the empirical pseudopotential spectrum (EPS) obtained without any s.o. coupling.[30] It follows from Fig. 7 that the peaks E_1 and E_2 are in good agreement with the EPS, whereas the peak E_1' in our curve is shifted to higher energy with respect to the EPS. The magnitudes of the peaks in the EPS are somewhat smaller, but at lower energies, $\hbar\omega \leq 6$ eV, our spectrum describes the experiment better, as follows from a comparison to Fig. 5(a).

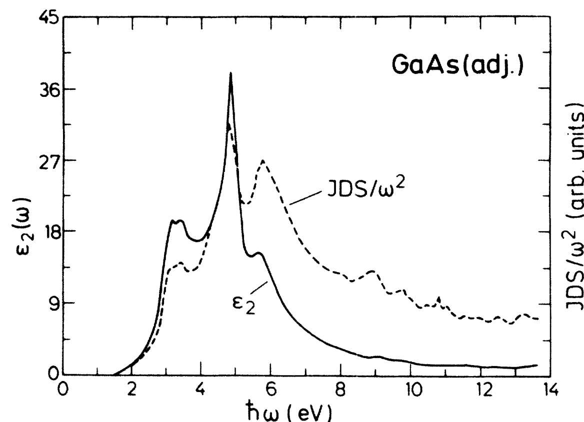

FIG. 6. Imaginary part $\epsilon_2(\omega)$ of the dielectric function of GaAs compared to the joint density of states (dashed curve) (JDS). The JDS is divided by ω^2 and scaled arbitrarily (factor A).

III. RESULTS AND DISCUSSION

The imaginary and real parts of the dielectric function between 0 and 13.6 eV for GaAs, Ge, InSb, and CdTe are shown in Figs. 5 and 8–10. The solid lines are theoretical results with the extra potentials added to the band structures. The experimental results included for comparison are the more recent ellipsometry measurements obtained by Cardona and co-workers.[29,31–33]

When the extra-potential correction (EPC) is included, our calculated dielectric functions are in good agreement with experiment. The calculated peak positions without EPC are too low in energy, as mentioned earlier, and

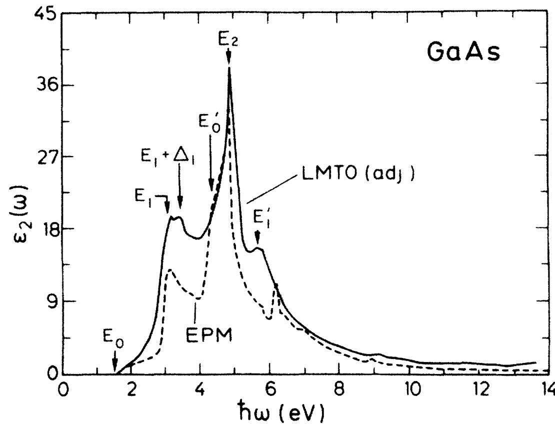

FIG. 7. Imaginary part $\epsilon_2(\omega)$ of the dielectric function of GaAs compared to the empirical pseudopotential spectrum (dashed curve) (Ref. 8).

they are even lower than those calculated by Wang and Klein.[23] This is due to the relativistic shifts which are included in our calculations but not in those of Ref. 23. It is a general feature of all theoretical spectra, that the intensity of the E_2 peak is overestimated and more sharply peaked than observed. This is so because $\epsilon_2(\omega)$ is calculated without inclusion of the effects of the finite

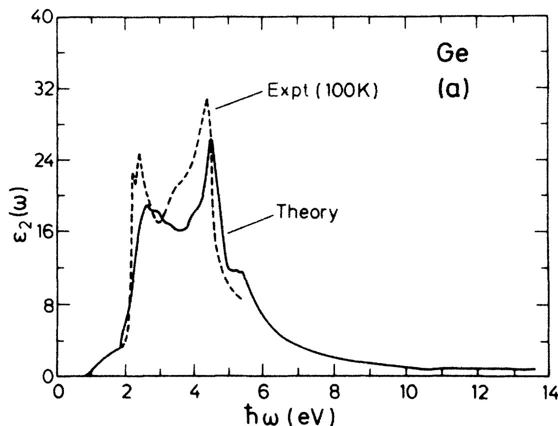

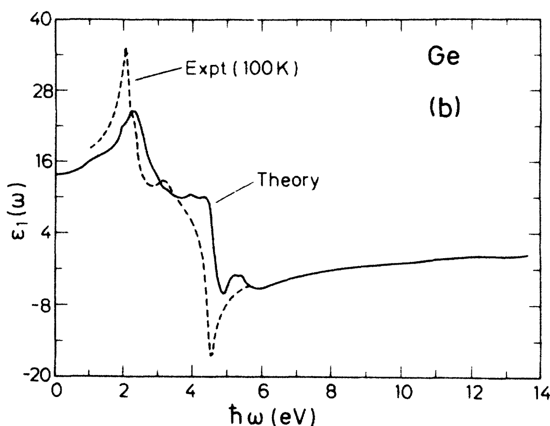

FIG. 8. Dielectric function of Ge with extra-potential corrections compared to the experimental results of Ref. 31 (dashed curves). (a) Imaginary part $\epsilon_2(\omega)$; (b) real part $\epsilon_1(\omega)$.

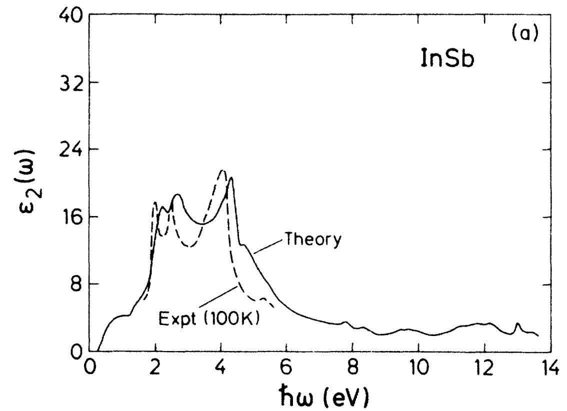

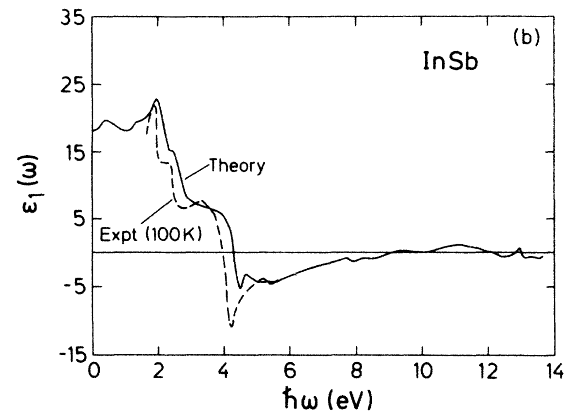

FIG. 9. As in Fig. 8, but for InSb. The experimental results are from Ref. 32.

relaxation time (many-body and excitonic effects). Also, surface effects may influence the peak heights in the experimental spectrum. Wang and Klein[23] have empirically introduced the effect of a finite relaxation time as a Lorentzian broadening in order to adjust the E_2 peak intensity to the experiment. This caused, however, the intensity of the E_1 peak to be too low.

The positions of all the peaks in $\epsilon_2(\omega)$, with a comparison to the experiment,[9,29,31–36] are given in Table I. In Table II we list the energy gaps at some critical points with comparison to the results from Chelikowsky and Cohen's[8] EPM calculation and also from the first-principles quasiparticle band-structure calculations available.[18,19] We have determined the regions in **k** space giving the major contributions to the intensity of the peaks of the $\epsilon_2(\omega)$. For that purpose we have examined the variation of the momentum matrix elements with **k**, and identified the tetrahedra where the contributions to the peaks in $\epsilon(\omega)$ are largest. For all four semiconductors studied here we find that essentially the same **k** points give rise to the major part of the intensity of the peaks. These regions will be specified below in the discussion of the GaAs data. We have also determined the most important interband contributions to the imaginary part of the dielectric function, which we show in Fig. 11 in the case of GaAs.

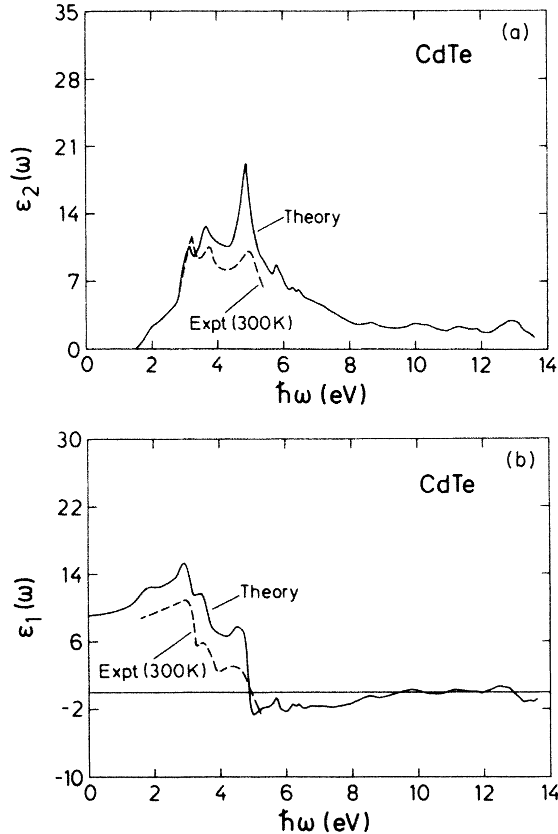

FIG. 10. As in Fig. 8, but for CdTe. The experimental results are from Ref. 33.

A. Gallium arsenide

The onset of the absorption edge (see Fig. 5) in the unadjusted $\epsilon_2(\omega)$ spectrum occurs at 0.20 eV, and at 1.51 eV in the adjusted one. This is the direct gap at Γ of GaAs. A low increase of $\epsilon_2(\omega)$ with photon energy $\hbar\omega$ is found as the band gap opens up away from Γ, but in the case of the unadjusted band, this increase near the edge is more rapid. This reflects the fact that the LDA band structure is not only in error by a constant shift of the conduction bands; the dispersion is also wrong.[12] In Fig. 11 the most important interband contributions to the peaks in $\epsilon_2(\omega)$ are shown. The $\epsilon_2(\omega)$ spectrum depicted in Fig. 11 is obtained without s.o. coupling in order to reduce the number of interband contributions to the essential ones. From Fig. 11 it is clear that the most important contribution to the E_1 and E_2 peaks is due to the transitions from the last valence band to the first conduction band. Ther is also a significant contribution from transition of band three to the first conduction band. The E_1' peak is split into two sharp peaks which are close to each other, and they originate from transitions from bands 3 and 4 to bands 5 and 6. In the ΓL direction near L, there is a large contribution to the $E1$ and $E1+\Delta_1$ peaks, but a region in the ΓLK plane [see Fig. 12(a)] also makes a significant contribution to these elements. The main peak, E_2, is arising principally from a region in the ΓXUL plane, where the bands are parallel. This region is shown in Fig. 12(b). A region similar to this was also found for germanium by Chelikowsky and Cohen.[8] We found also a contribution to the E_2 peak in the ΓK direction in the neighborhood of K (see Fig. 1). The contribution to the shoulder E_0' is very difficult to define exactly, but the main contribution seems to come from a region in the vicinity of the Γ point, $\Gamma_8^v \rightarrow \Gamma_7^c$ transitions. At higher energy, the peak E_1' is mainly due to transitions $\Delta_5^v \rightarrow \Delta_5^c$ in the ΓX direction. The structure element E_1' is not present in the experimental ellipsometry data because of its limitation in photon energy, but this peak is seen in the reflectivity measurement as obtained by Philipp and Ehrenreich.[34] Our E_1' peak is somewhat downshifted in energy with respect to the experiment[34] and EPS.[9] This is due to the fact that our band gap at X is smaller than observed (see Table II). At still higher energy the theoretical spectrum is without structures and decays very rapidly with photon energy. This rapid decay agrees well with experiment[34] and allows the spectrum to satisfy the f-sum rule.

The real part of $\epsilon(\omega)$, $\epsilon_1(\omega)$, shown in Fig. 5(b) is in

TABLE I. Calculated peak positions (in eV) in $\epsilon_2(\omega)$ for the GaAs, Ge, InSb, and CdTe, with comparison to experiment.

	GaAs		Ge		InSb		CdTe	
Semiconductor	Theor.	Expt.	Theor.	Expt.	Theor.	Expt.	Theor.	Expt.
E_0	1.51	1.51[a]	0.85	0.89[c]	0.24	0.24[c]	1.51	1.50[h]
E_1	3.16	3.04[a]	2.69	2.10[d]	2.24	1.98[f] 1.97[g]	3.16	3.35[h]
Δ_1	0.22	0.22[a]	0.17	0.19[d]	0.45	0.50[g]	0.48	0.55[h]
$E_1+\Delta_1$	3.38	3.26[a]	2.86	2.30[e]	2.69	2.49[g] 2.48[f]	3.64	3.90[h]
E_2	4.83	5.13[a]	4.56	4.35[d]	4.28	4.23[f] 4.18[g]	4.83	5.00[h]
E_1'	5.60	6.20[b]	5.24	5.70[b]	4.62	5.00[b] 5.22[g]	5.76	

[a]From Lautenschlager *et al.* (Ref. 29).
[b]Philipp and Ehrenreich (Ref. 34).
[c]Harrison (Ref. 9).
[d]Viña *et al.* (Ref. 31).
[e]Aspnes and Rowe (Ref. 35).
[f]Zucca and Shen (Ref. 36).
[g]Logothetidis *et al.* (Ref. 32).
[h]Lautenschlager *et al.* (Ref. 33).

TABLE II. Energy gaps (in eV) at critical points for GaAs, Ge, InSb, and CdTe with comparison to the empirical pseudopotential results and to the first-principles quasiparticle band-structure calculations. For Ge, Γ_6^c and Γ_7^c are inverted and X_6 and X_7 are gathered into X_5 by symmetry. (The numbers without labels are our calculations including the adjusting external potentials.)

Semiconductor	GaAs	Ge	InSb	CdTe
Γ_6^c-Γ_8^v	1.51, 1.51,[a] 1.58[b]	0.85, 0.90,[a] 0.75[c]	0.24, 0.25[a]	1.51, 1.59[a]
Γ_6^c-Γ_7^v	1.76, 1.86[a]	1.16, 1.19[a] 1.05[c]	1.01, 1.07[a]	2.35, 2.48[a]
Γ_7^c-Γ_8^v	3.66, 4.55[a]	2.84, 3.01,[a] 3.04[c]	2.65, 3.16[a]	4.29, 5.36[a]
L_6^c-$L_{4,5}^v$	2.74, 3.02,[a] 3.04[b]	2.19, 2.19[a]	1.91, 1.99[a]	2.92, 3.47[a]
L_6^c-L_6^v	2.95, 3.24[a]	2.38, 2.39[a]	2.40, 2.47[a]	3.45, 4.00[a]
Δ_1	0.21, 0.22[a]	0.19, 0.20,[a] 0.18[c]	0.49, 0.48[a]	0.53, 0.53[a]
X_6^c-X_7^v	4.69, 4.92[a] 4.83[b]	4.59, 4.45[a] 4.45[c]	4.23, 3.95[a]	4.63, 5.08[a]
X_6^c-X_6^v	4.77, 5.02[a]	4.59, 4.45[a] 4.45[c]	4.40, 4.16[a]	4.96, 5.46[a]

[a]Empirical pseudopotential calculation of Ref. 8.
[b]First-principles quasiparticle band-structure calculation of Ref. 19.
[c]First-principles quasiparticle band-structure calculation of Ref. 18.

good agreement with the experiment[29] when the EPC is applied (solid curve). Our results are a one-electron calculation, suggesting that deviations from the experimental amplitudes and peak positions can be attributed to many-body effects. The empirical nature of our corrections (EPC) to the band structure will of course be responsible for a large part of the difference between the theoretical and the experimental spectrum. The calculated static dielectric constant is 12.95, and without EPC this value is 14.90. The experimental value is 10.9.[37] The two calculated numbers reflect the fact that when the peaks in $\epsilon_2(\omega)$ are shifted to lower energies then the $\epsilon(0)$ is enhanced.

Hanke and Sham[14] (HS) and Louie *et al.*[16] found that local-field effects decrease the value of $\epsilon(0)$ for silicon by 1.87 (HS , Refs. 14) and 1.1 (Louie *et al.*[16]), respectively. Subtracting terms of this order of magnitude (1–2) from our $\epsilon(0)$ value, a result close to the experiment is obtained. There are, however, several effects which are not included in our calculation. Excitonic effects, electron-phonon interactions, and other many-body corrections may thoroughly influence ϵ_1 also at zero frequency. At finite frequencies below 2.5 eV we find the same order of magnitude of the difference between our calculated ϵ_1 values and experiments. This is seen, for example, in Table III, where we compare our results at $\hbar\omega=1.5$ to the experimental data obtained by Aspnes and Studna.[38]

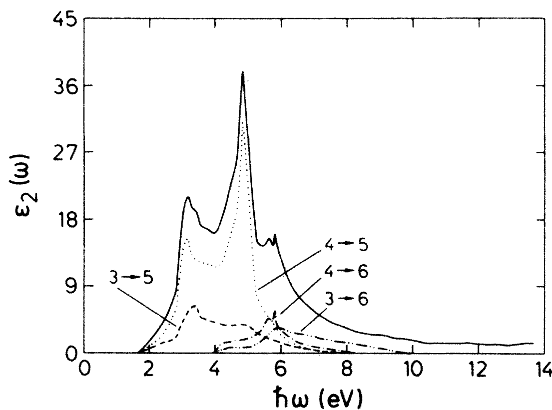

FIG. 11. The most important interband contributions to the imaginary part of the dielectric function of GaAs. (Spin-orbit coupling is not included.)

B. Germanium

We discuss only briefly the results of Ge, since this elemental semiconductor has previously been extensively studied.[2,6,9,23,31,34,35] The peak positions are compared to experiment in Table I. The critical-point energy differences are given in Table II and they are in good agreement with the EPM results.[8] The onset of the absorption occurs at 0.85 eV (calculated with EPC), corresponding in our calculation to the direct band gap at Γ (we include only direct transitions). The peaks E_1, $E_1+\Delta_1$, E_0', E_2, and E_1' have their origin in the same region of **k** space as those of GaAs. It follows from Fig. 8 that the intensity of the calculated peaks is less than observed.[31] This is the only case among those examined here where the E_2 peak is lower than what is observed.[31] The reason for that is the shift towards higher energy of the calculated peaks with respect to the experiment.[31] This also explains why our value of $\epsilon(0)$, 14.08, is smaller than measured (15.8).[39] We would, as mentioned in the preceding subsection, expect the calculated value to be slightly larger than measured.

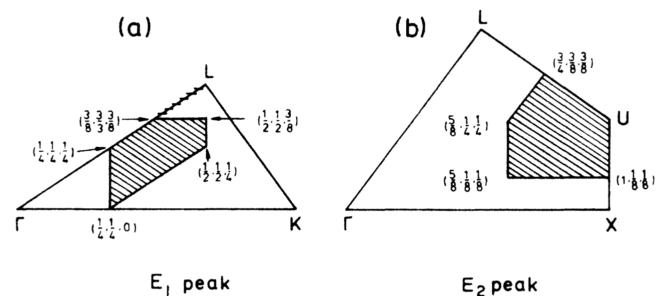

FIG. 12. Regions in the **k** space which contribute to the E_1, $E_{1s}(E_1+\Delta_1)$, and E_2 peaks of $\epsilon_2(\omega)$ of GaAs. (a) E_1, E_{1s} peak regions; (b) E_2 peak region.

TABLE III. Real part $\epsilon_1(\omega)$ of the dielectric function at 1.5 eV compared to experiment. Values in the row labeled "Expt." are ellipsometry measurements from Ref. 38.

Semiconductor	GaAs	Ge	InSb	CdTe
Expt.	13.44	21.56	19.11	
Theor.	15.36	18.20	19.00	10.66

C. Indium antimonide

The dielectric function of InSb (see Fig. 9) is very similar to that of GaAs. The positions of the peaks are listed in Table I, with comparison to experiments. The critical-point gaps (see Fig. 3) are close to those obtained by means of EPM (Ref. 8) (see Table II). The real part of ϵ, $\epsilon_1(\omega)$, is shown in Fig. 9(b). It is seen that all the experimental structure elements[32] are present in the calculated spectrum. Even the intensity of the peaks is in good agreement with the experiment.

The static dielectric constant $\epsilon(0)$ is found to be 17.87, whereas the experimental value is about 15.7.[9] This difference is probably mainly due to the neglect of the local-field effect.[14–16]

D. Cadmium telluride

The imaginary and real parts of the dielectric function of CdTe are shown in Fig. 10. The experimental spectrum[33] is also depicted in the same figure. The peak positions are given in Table I, as for the other semiconductors. The critical-point energies shown in Table II for CdTe are somewhat smaller than the EPM values.[9] The identification of the regions in the **k** space where the main structure elements occur is similar to that found for the other semiconductors, including the E_1' peak. In the high-energy part of the spectrum, two peaks, at 6.2 and 6.5 eV, are found near E_1'. We identify them with those obtained by Chadi *et al.*,[3] in their measurement of the reflectivity spectra, at 5.95 and 6.82 eV. Their[3] structure elements at 7.44 and 7.6 eV may correspond to our shoulder near 8.5 eV. We obtained also a small structure at the higher part of the spectrum where no experimental data are available. The calculated $\epsilon_1(\omega)$ is compared in Fig. 10(b) to the experimental spectra of Lautenschlager *et al.*[33] The positions of the peaks are in good agreement with experiment, but the intensity of the E_2 peak is somewhat overestimated. Since our $\epsilon_2(\omega)$ spectrum satisfies the f-sum rule, we suggest that the experimental spectrum, which obviously cannot fulfill this, may be somewhat in error. Further, for all the semiconductors that we have studied we find that the intensity of the E_2 peak is higher than that of the E_1 peak. Even in the EPM calculation[3] the E_2 peak intensity is higher than that of the E_1 peak and in good agreement with the amplitudes in our spectrum. In general the comparison of theory and experiment is further complicated by the fact that the preparation and maintenance of samples of high quality are difficult, and imperfections may affect the experimental data appreciably.[40] The study by Vedam and So,[41] for example, shows clearly the effects of different surface treatments in the optical parameters of silicon.

The calculated static dielectric constant $\epsilon(0)$ of CdTe is found to be 9.11, where the experimental value is 7.3.[9] As for the InSb, this difference is due mainly to the local field not taken into account in our calculation.

E. Gallium arsenide under pressure

The imaginary part of the dielectric function of GaAs for several values of the lattice constant are presented in Fig. 13. From this figure we observe that all peaks move towards higher energies when the pressure increases. The positions of the peaks under pressure and their pressure dependence compared to experiments[42–45] are listed in Table IV. Since their origins in **k** space remain unchanged under hydrostatic pressure, the shifts of the peaks to higher energy are due to the increase of the band gaps, as illustrated in Fig. 14. This also explains the increase of the optical gap under pressure. From Table IV it is seen that $\epsilon(0)$ decreases when the pressure increases.

The logarithmic derivative $d\ln E_2/d\ln d$, where d is the bond length, is found to be -1.85. This agrees well with the value -1.5 predicted by Harrison[46] for semiconducting III-V compounds. We do not find that the susceptibility varies linearly with the bond length as suggested by the same author for the elemental semiconductors. Our value of the logarithmic derivative $d\ln\epsilon(0)/d\ln d$ of the static dielectric constant $\epsilon(0)$ is equal to 5.85. Measurements by Kastner[47] support, to some extent, our value for GaAs, since this author found 2.2 for diamond, 2 for silicon, 4.6 for germanium, and 3.6 for GaAs.

Based on our bond-length scaling of E_2, $d^{-1.85}$, and $\epsilon(0)$, $d^{4.85}$, and assuming that the main contribution to $\epsilon(0)$ comes from an energy region around the E_2 peak, a

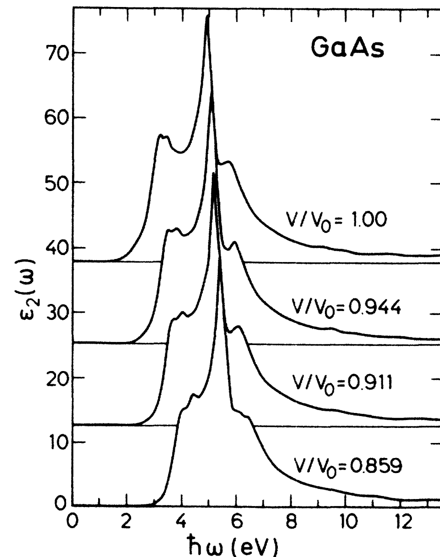

FIG. 13. Dielectric function of GaAs for different volumes V. (V_0 is the equilibrium volume.)

TABLE IV. Calculated peak positions in the $\epsilon_2(\omega)$, static dielectric function $\epsilon(0)$, and electronic pressure P of GaAs for different lattice parameters, a. The last column gives the linear pressure coefficients as calculated from the theoretical equation of state with a comparison to available experimental data.

	a (Å)				dE/dP (eV/Mbar)	
	5.66	5.55	5.49	5.38	Theor.	Expt.
E_0 (eV)	1.51	2.06	2.36	2.86	12.3	11.1[a] 12.6[b] 10.8[c]
E_1 (eV)	3.16	3.50	3.71	4.05	7.76	7.1[a] 7.5[d]
Δ_1 (eV)	0.22	0.27	0.30	0.34	0.77	0.2[a]
E_{1s} (eV)	3.38	3.77	4.01	4.39	8.53	7.3[a] 7.6[d]
E_2 (eV)	4.83	5.00	5.13	5.34	3.96	5.6[d]
E_1' (eV)	5.64	5.92	5.92	5.92	6.89	
$\epsilon(0)$	12.95	11.51	10.87	9.96		
P (kbar)	−1.17	46.16	81.79	157.7		

[a]Thermomodulation (Ref. 42).
[b]Transmission, diamond-anvil cell (Ref. 43).
[c]Optical absorption under pressure, diamond-anvil cell (Ref. 44).
[d]Reflectance (Ref. 45).

crude estimate of $\epsilon(0)$ could be obtained as

$$\epsilon(0) \propto \frac{1}{\Omega} \frac{\langle P^2 \rangle}{E_2^3} , \tag{2}$$

with

$$\langle P^2 \rangle = \sum_{\mathbf{k},n,n'} | \langle n\mathbf{k} | \mathbf{P} | n'\mathbf{k} \rangle |^2 . \tag{3}$$

Here $\mathbf{k}$ is limited to the region of reciprocal space such that

$$E_2 - \delta E \le E_{n'}^{\mathbf{k}} - E_n^{\mathbf{k}} \le E_2 + \delta E , \tag{4}$$

where δE is a small positive energy. We find that $d \ln\langle P^2 \rangle^{1/2} / d \ln d$ is equal to 1.65. If, on the other hand, we suppose that $d \ln\epsilon(0)/d \ln d$ is equal to one, as suggested by Harrison,[46] then $d \ln\langle P^2 \rangle^{1/2}/d \ln d$ would be equal to -1, in good agreement with the scaling obtained recently by Brey *et al.*[48] But this is fortuitous since $\epsilon(0)$ is not just dependent on the contribution around the E_2 peaks. A careful analysis of our momentum matrix elements for transitions in the regimes of E_1, $E_1+\Delta_1$, and E_2 peaks shows that we found a scaling similar to that of Ref. 48. We have defined an average of the momentum matrix elements:

$$\langle P^2 \rangle = \frac{1}{N} \sum_{\mathbf{k} \in \text{zone}; n,n'} | \langle n\mathbf{k} | \mathbf{P} | n'\mathbf{k} \rangle |^2 , \tag{5}$$

for the E_1, $E_1+\Delta_1$, and E_2 peaks. Here "zone" stands for the $\mathbf{k}$-space region where peak E_1 or E_2 originates, N is the total number of transitions giving rise to the peak, and n,n' are the indices of the occupied and unoccupied bands, respectively, having a difference in energy equal to the photon energy. We find that the matrix elements increase with increasing pressure as shown in Table V and it follows that $d \ln\langle P^2 \rangle^{1/2}/d \ln d$ is equal to -0.5 for the E_1 and the $E_1+\Delta_1$ peaks, and -0.91 for the E_2 peak.

Characteristic energy gaps calculated for GaAs at four different lattice constants are given in Table VI. As mentioned earlier, the parameters used in the EPC are kept pressure independent. Using the theoretical equation of state we calculate (fifth column of Table VI) the pressure coefficients. The first-order coefficients are in excellent agreement with experiments.[42–44,49,50] A more-detailed test of the calculated equation of state involves a comparison of theoretical and experimental values of higher-order pressure coefficients.[51] It is of further interest to note the differences between the pressure coefficients for the critical-point energies (Table VI) and those of the peaks in $\epsilon_2(\omega)$ (Table IV), in particular for E_1 and $E_1+\Delta_1$.

F. Germanium under pressure

The imaginary part of the dielectric function of Ge for several values of the lattice constant, chosen in the semiconducting phase, are presented in Fig. 15. From this figure, as in the case of GaAs, we observe that all the peaks move towards higher energies when the pressure increases. The positions of the peaks under pressure and their pressure dependence compared to experiments[45,52] are listed in Table VII. As for GaAs, the change in band structure which explains these shifts is illustrated in Fig. 16. From Table VII it is seen that $\epsilon(0)$ decreases under compression of the lattice. We found that $d \ln\epsilon(0)/d \ln d$ is equal to 1.38, which is far from the value of 4.6 measured by Kastner[47] but is in good agreement with the linearity variation predicted by Harrison[46] for the elemental semiconductors. The pressure depen-

FIG. 14. Band structure of GaAs in the gap regime for different volumes V. (V_0 is the equilibrium volume.)

dences of the direct and indirect band gaps are found to be 12.5 and 4.38 eV/Mbar, respectively, in good agreement with experimental results of 12.5 and 3 eV/Mbar obtained by piezoelectroreflectance[52] and piezotransmission,[53] respectively. For the calculation of those pressure coefficients we did use the experimental bulk modulus as obtained by Bruner and Keyes[54] because we did not calculate the pressure volume relation for Ge. In Table VIII we present our calculated band gaps for Ge

TABLE V. Average values of the square of the momentum matrix elements (in atomic units) for the E_1 and E_2 peaks of GaAs at different lattice parameters, a.

	a (Å)			
	5.66	5.55	5.49	5.38
$\langle P_{E1}^2 \rangle$	0.570	0.581	0.596	0.596
$\langle P_{E2}^2 \rangle$	0.610	0.631	0.641	0.667

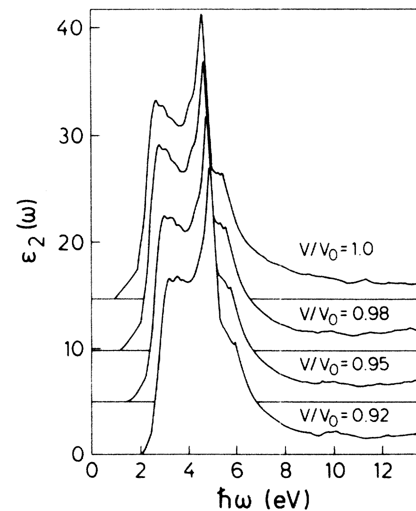

FIG. 15. Dielectric function of Ge for different volumes V. (V_0 is the equilibrium volume.)

TABLE VI. Energy-band gaps (in eV) in GaAs for different lattice constants, a. The fifth column gives the linear pressure coefficients as calculated from the theoretical equation of state. Experimental available values of pressure coefficients are also given in the last column. The coefficients for E_1 and E_{1s} should be compared to our calculated values for L_6^c-$L_{4,5}^v$ and L_6^c-L_6^v, respectively. (The same parameters of the correcting potentials were used at all four volumes.)

	a (Å)				dE/dP (eV/Mbar)	
	5.66	5.55	5.49	5.38	Theor.	Expt.
Γ_6^c-Γ_8^v	1.51	2.06	2.36	2.86	12.3	11.1[a]
	1.43[b]	1.95[b]	2.25[b]	2.83[b]		12.6[c]
						10.8[b]
Γ_6^c-Γ_7^v	1.76	2.31	2.61	3.13	12.2	12.7[d]
Γ_7^c-Γ_8^v	3.66	3.69	3.70	3.71	0.50	
L_6^c-$L_{4,5}^v$	2.74	3.06	3.25	3.59	7.10	7.1[a]
L_6^c-L_6^v	2.95	3.27	3.47	3.82	7.20	7.3[a]
Δ_1	0.21	0.21	0.22	0.23	0.1	0.2[a]
X_6^c-X_7^v	4.69	4.84	4.94	5.11	3.40	
X_6^c-X_6^v	4.77	4.92	5.02	5.19	3.40	
X_6^c-Γ_8^v	1.91	1.86	1.83	1.68	−1.15	−1.35[b]
	1.93[b]	1.83[b]	1.78[b]	1.52[b]		−1.8[e]

[a]Thermomodulation (Ref. 42).
[b]Optical absorption under pressure, diamond-anvil cell (Ref. 44).
[c]Transmission, diamond-anvil cell (Ref. 43).
[d]Luminescence average, diamond-anvil cell (Ref. 49).
[e]Electroreflectance (Ref. 50).

TABLE VII. Peak positions in the $\epsilon_2(\omega)$, static dielectric function $\epsilon(0)$ of Ge for different lattice parameters, a. The last columns give the linear pressure coefficients with a comparison to available experimental data.

	a (Å)				dE/dP (eV/Mbar)	
	5.66	5.62	5.57	5.51	Theor.	Expt.
E_0 (eV)	0.85	1.05	1.40	1.73	12.5	12.5[a]
E_1 (eV)	2.69	2.80	2.99	3.19	6.89	7.5[b]
Δ_1 (eV)	0.21	0.24	0.30	0.34	1.88	
E_{1s} (eV)	2.90	3.04	3.30	3.54	8.77	
E_2 (eV)	4.56	4.66	4.76	4.86	6.27	5.6[b]
E_1' (eV)	5.40	5.54	5.70	5.92	8.77	
$\epsilon(0)$	14.08	13.71	12.30	11.49		

[a]Piezoelectroreflectance (Ref. 52).
[b]Reflectance (Ref. 45).

TABLE VIII. Energy-band gaps in Ge for different lattice constants, a. The sixth column gives the linear pressure coefficients; experimental available values of pressure coefficients are also given in the last column.

	a (Å)				dE/dP (eV/Mbar)	
	5.66	5.62	5.57	5.51	Theor.	Expt.
Γ_7^c-Γ_8^v	0.85	1.05	1.40	1.73	12.3	12.5[a]
	0.80[b]	0.99[b]	1.32[b]	1.72[b]		12.1[b]
Γ_7^c-Γ_7^v	1.16	1.37	1.72	2.05	12.5	12.3[b]
	1.08[b]	1.33[b]	1.70[b]	2.06[b]		
Γ_6^c-Γ_8^v	2.84	2.86	2.88	2.90	1.25	
L_6^c-$L_{4,5}^v$	2.19	2.30	2.50	2.69	6.89	7.5[c]
L_6^c-L_6^v	2.38	2.50	2.70	2.89	7.52	
Δ_1	0.19	0.20	0.20	0.21	0.63	
X_5^c-X_5^v	4.59	4.70	4.82	4.93	3.76	
L_6^c-Γ_8^v	0.82	0.89	1.04	1.17	4.38	3.0[d]

[a]Piezoelectroreflectance (Ref. 52).
[b]Optical absorption under pressure, diamond-anvil cell (Ref. 55).
[c]Reflectance (Ref. 45).
[d]Piezotransmission (Ref. 53).

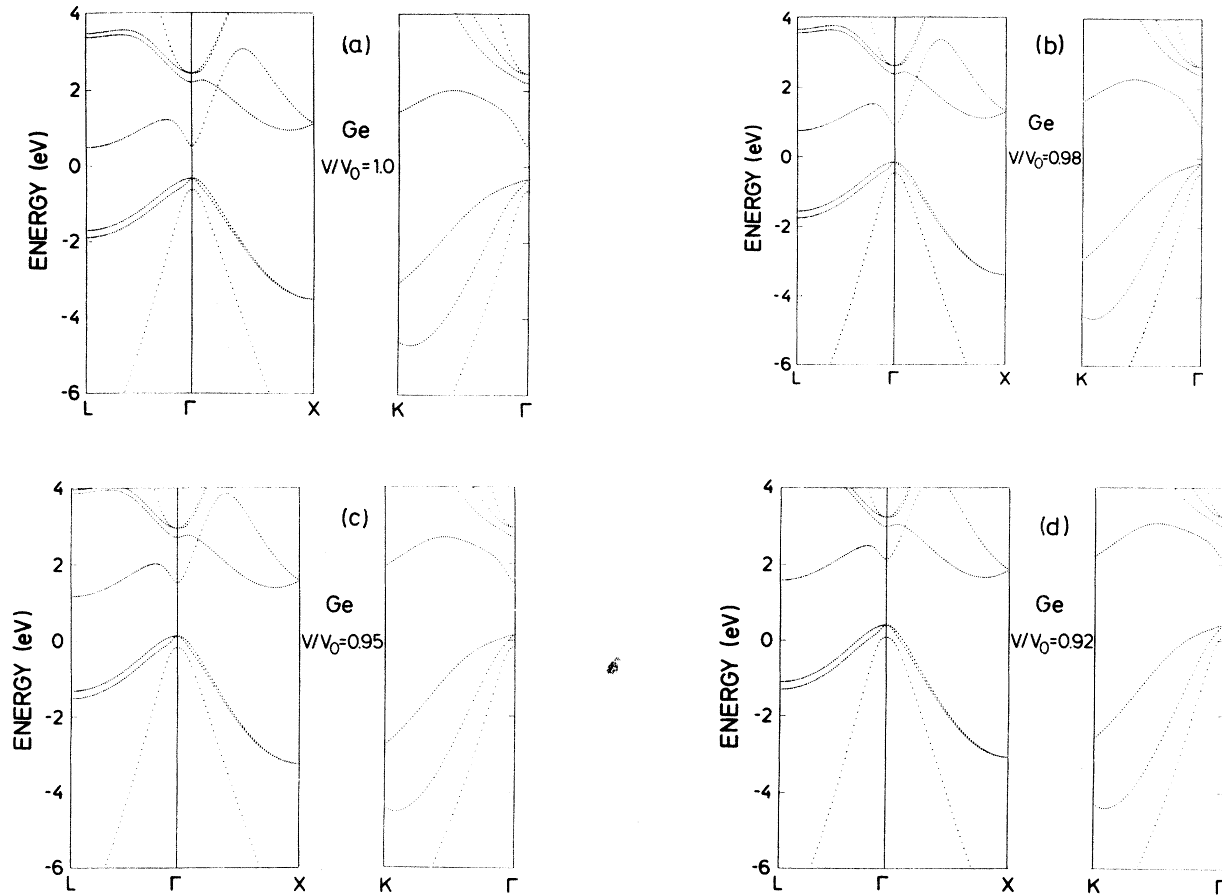

FIG. 16. Band structure of Ge in the gap regime for different volumes V. (V_0 is the equilibrium volume.)

and their first-order pressure coefficients compared to the available experimental results,[45,52,53,55] and we also compare in the same table the direct gap and the s.o. splitting Δ_0 at Γ for several values of the lattice constant with the data obtained by Goñi *et al.*[55] As we can see from Table VIII, a good agreement with experiment is obtained.

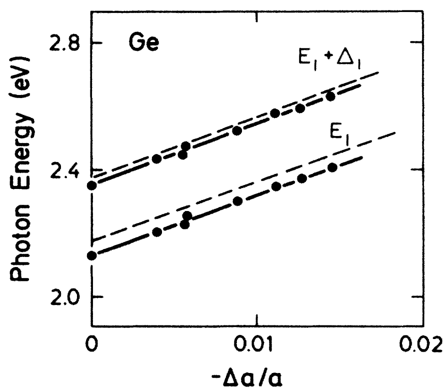

FIG. 17. Evolution of the E_1 and $E_1+\Delta_1$ band gaps of Ge under compression of the lattice. (Δa is the change of the lattice parameter a.) The experimental results (solid curves) are from Ref. 56.

The evolution of the $E_1(L_6^c-L_{4,5}^v)$ and $E_1+\Delta_1(L_6^c-L_6^v)$ critical-point energy differences under compression, with comparison to the results of Kobayashi *et al.*[56] as obtained from their thermoreflectance spectra of Ge, is depicted in Fig. 17. The calculated E_1 gap is slightly larger than measured but their evolution under compression is linear and has the same slope as observed. In general, there is a good agreement of the pressure dependence of the calculated gaps and optical peaks with experiment (see Table VIII) but the absolute values of the calculated E_1 and $E_1+\Delta_1$ optical peaks are slightly larger than measured.

IV. CONCLUSION

The dielectric functions of GaAs, Ge, InSb, and CdTe have been obtained by means of the LMTO method. The relativistic effects drastically reduce the optical band gaps and shift all peak positions to lower energy with respect to nonrelativistic calculations[23] and experiments.[29,31–33] External potentials are added to the local-density potential in order to introduce "artificial Darwin shifts" for adjusting the band gaps to the experiment. Self-consistent band structures obtained in this way give satisfactory results when used to calculate the optical spectra of semiconductors. All the peak posi-

tions and the spin-orbit splitting Δ_1 are in good agreement with the experimental data. The difference in the intensity of the peaks calculated and observed is due mainly to the many-body effects not taken into account in our calculation.

We predicted the effect of hydrostatic pressure on the electronic structure and optical properties of GaAs and Ge, and found that the structures in the dielectric function shift towards higher energies when the pressure increases. The static dielectric constant decreases with pressure. The scaling with interatomic distance of the E_2 peak, static dielectric constant, and average momentum matrix element are in good agreement with the available theoretical and experimental results. The calculated pressure coefficient for band gaps is in good agreement with the experimental data. The pressure coefficients for the peaks in $\epsilon_2(\omega)$ are in some cases significantly different from those of the critical-point band gaps. Thus an accurate extraction of pressure coefficients of band gaps from experimental data must involve a careful line-shape analysis.

ACKNOWLEDGMENTS

We are grateful to K. Syassen for several helpful discussions concerning our calculations. One of us (L.B.) thanks the Max Planck Institute for its hospitality during a visit in Stuttgart and Comunidad Autónoma de Madrid for financial support in connection with this visit.

---

*Permanent address: Departemento Fisica Estado Solido Facultad Ciencias, Universidad Autónoma, Madrid, Spain.

[1]T. C. Collins, D. J. Stukel, and R. N. Euwema, Phys. Rev. B **1**, 724 (1970).

[2]M. L. Cohen and V. Heine, in *Solid State Physics*, edited by F. Seitz, D. Turnbull, and H. Ehrenreich (Academic, New York, 1970), Vol. 24, p. 37.

[3]D. J. Chadi, J. P. Walter, M. L. Cohen, Y. Petroff, and M. Balanski, Phys. Rev. B **5**, 3058 (1972).

[4]R. Pollak, L. Ley, S. Kowalcyzk, D. A. Shirley, J. Joannapoulos, D. J. Chadi, and M. L. Cohen, Phys. Rev. Lett. **29**, 1103 (1973).

[5]J. D. Joannapoulos and M. L. Cohen, Phys. Rev. B **8**, 2733 (1973).

[6]J. R. Chelikowsky and M. L. Cohen, Phys. Rev. Lett. **31**, 1582 (1973).

[7]W. D. Grobman, D. E. Eastman, and J. L. Freeouf, Phys. Rev. B **12**, 4405 (1975).

[8]J. R. Chelikowsky and M. L. Cohen, Phys. Rev. B **14**, 556 (1976).

[9]W. A. Harrison, *Electronic Structure and the Properties of Solids* (Freeman, San Francisco, 1980).

[10]C. S. Wang and B. M. Klein, Phys. Rev. B **24**, 3393 (1981).

[11]N. E. Christensen, Phys. Rev. B **30**, 5753 (1984).

[12]G. B. Bachelet and N. E. Christensen, Phys. Rev. B **31**, 879 (1985).

[13]N. E. Christensen and O. B. Christensen, Phys. Rev. B **33**, 4739 (1986).

[14]W. R. Hanke and L. J. Sham, Phys. Rev. Lett. **33**, 582 (1974).

[15]W. R. Hanke and L. J. Sham, Phys. Rev. B **21**, 4656 (1980).

[16]S. G. Louie, J. R. Chelikowsky, and M. L. Cohen, Phys. Rev. Lett. **34**, 155 (1975).

[17]M. S. Hybertsen and S. G. Louie, Phys. Rev. Lett. **55**, 1418 (1985); R. W. Godby, M. Schlüter, and L. J. Sham, Phys. Rev. Lett. **56**, 2415 (1986).

[18]M. S. Hybertsen and S. G. Louie, Phys. Rev. B **34**, 5390 (1986).

[19]R. W. Godby, M. Schlüter, and L. J. Sham, Phys. Rev. Lett. **56**, 2415 (1986).

[20]C. S. Wang and W. E. Pickett, Phys. Rev. Lett. **51**, 597 (1983).

[21]D. Straub, L. Ley, and F. J. Himpsel, Phys. Rev. Lett. **54**, 142 (1985).

[22]A. Fleszar and R. Resta, Phys. Rev. B **31**, 5305 (1985).

[23]C. S. Wang and B. M. Klein, Phys. Rev. B **24**, 3417 (1981).

[24]O. K. Andersen, Phys. Rev. B **12**, 3060 (1975).

[25]F. Szmulkowicz and B. Segall, Phys. Rev. B **24**, 892 (1981).

[26]M. Alouani, J. M. Koch, and M. A. Khan, J. Phys. F **16**, 473 (1986).

[27]O. Jepsen and O. K. Andersen, Solid State Commun. **9**, 1763 (1971); G. Lehman and M. Taut, Phys. Status Solid B **54**, 469 (1972).

[28]Y. Petroff, M. Balkanski, J. P. Walter, and M. L. Cohen, Solid State Commun. **7**, 459 (1968).

[29]P. Lautenschlager, M. Garriga, S. Logothetidis, and M. Cardona, Phys. Rev. B **35**, 9174 (1987).

[30]See M. L. Cohen and V. Heine, in *Solid State Physics*, Ref. 2, p. 142.

[31]L. Viña, S. Logothetidis, and M. Cardona, Phys. Rev. B **30**, 1979 (1984).

[32]S. Logothetidis, L. Viña, and M. Cardona, Phys. Rev. B **31**, 947 (1985).

[33]P. Lautenschlager, S. Logothetidis, L. Viña, and M. Cardona, Phys. Rev. B **32**, 3811 (1985).

[34]H. R. Phillipp and H. Ehrenreich, Phys. Rev. **129**, 1550 (1963).

[35]D. E. Aspnes and J. E. Rowe, Phys. Rev. B **7**, 887 (1973).

[36]R. R. Zucca and Y. R. Shen, Phys. Rev. B **1**, 2668 (1976).

[37]M. Hase and B. W. Henris, J. Phys. Chem. Solids **23**, 1099 (1962).

[38]D. E. Aspnes and A. A. Studna, Phys. Rev. B **27**, 985 (1983).

[39]C. Kittel, *Introduction to Solid State Physics* (Wiley, New York, 1976), p. 309.

[40]D. E. Aspnes and A. A. Studna, Appl. Phys. Lett. **39**, 316 (1981).

[41]K. Vedam and S. S. So, Surf. Sci. **29**, 379 (1972).

[42]M. Hanfland, K. Syassen, and N. E. Christensen, J. Phys. (Paris) Colloq., Suppl. 11 **45**, C8-57 (1984); M. Hanfland and K. Syassen (private communication).

[43]B. Welber, M. Cardona, M. Kim, and C. K. Rodriguez, Phys. Rev. B **12**, 5729 (1975).

[44]A. R. Goñi, K. Strössner, K. Syassen, and M. Cardona, Phys. Rev. B **36**, 1581 (1987).

[45]R. Zallen and W. Paul, Phys. Rev. **155**, 703 (1967).

[46]See W. A. Harrison, *Electronic Structure and the Properties of Solids*, Ref. 9, p. 110.

[47]M. Kastner, Phys. Rev. B **6**, 2273 (1972).
[48]L. Brey, C. Tejedor, and J. A. Vérges, Phys. Rev. B **29**, 6840 (1984).
[49]D. Olego, M. Cardona, and H. Müller, Phys. Rev. B **22**, 894 (1980).
[50]R. Bendoruis and A. Shileika, Solid State Commun. **8**, 616 (1970).
[51]M. Hanfland, K. Syassen, and N. E. Christensen (unpublished).
[52]F. H. Pollak and M. Cardona, Phys. Rev. **172**, 816 (1968).
[53]I. Balslev, Phys. Rev. **143**, 636 (1966).
[54]L. J. Bruner and R. W. Keyes, Phys. Rev. Lett. **7**, 55 (1961).
[55]A. R. Goñi, K. Strössner, K. Syassen, and M. Cardona (unpublished).
[56]M. Kobayashi, T. Nagahawa, and Y. Nisida, in *Proceedings of the International Conference on the Physics of Semiconductors, Stockholm, 1986,* edited by O. Engström (World Scientific, Singapore, 1987), p. 1153.